Advanced Structured Materials

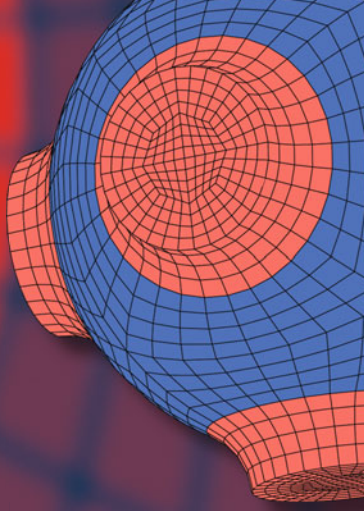

Andreas Öchsner
Holm Altenbach *Editors*

# Mechanical and Materials Engineering of Modern Structure and Component Design

Springer

# Advanced Structured Materials

Volume 70

More information about this series at http://www.springer.com/series/8611

Andreas Öchsner · Holm Altenbach
Editors

# Mechanical and Materials Engineering of Modern Structure and Component Design

Springer

*Editors*
Andreas Öchsner
Griffith School of Engineering
Griffith University
Southport Queensland, QLD
Australia

and

The University of Newcastle
Callaghan, QLD
Australia

Holm Altenbach
Fakultät für Maschinenbau, Lehrstuhl für Technische Mechanik
Institut für Mechanik
Otto-von-Guericke-Universität Magdeburg
Magdeburg
Germany

ISSN 1869-8433 ISSN 1869-8441 (electronic)
Advanced Structured Materials
ISBN 978-3-319-19442-4 ISBN 978-3-319-19443-1 (eBook)
DOI 10.1007/978-3-319-19443-1

Library of Congress Control Number: 2015939927

Springer Cham Heidelberg New York Dordrecht London


Printed on acid-free paper

Springer International Publishing AG Switzerland is part of Springer Science+Business Media (www.springer.com)

# Preface

The idea of this monograph is to present the latest results related to mechanical and materials engineering applied to the design of modern engineering materials and components. The contributions cover the classical fields of mechanical, civil, and materials engineering up to bioengineering and advanced materials processing and optimization. The materials and structures covered can be categorized into modern steels, aluminum and titanium alloys, polymers/composite materials, biological and natural materials, material hybrids, and modern nano-based materials. Analytical modeling, numerical simulation, the application of state-of-the-art design tools, and sophisticated experimental techniques are applied to characterize the performance of materials and to design and optimize structures in different fields of engineering applications.

The 8th International Conference on Advanced Computational Engineering and Experimenting, ACE-X 2014, was held in Paris, France, from June 30, 2014 to July 3, 2014 with a strong focus on computational-based and supported engineering. This conference served as an excellent platform for the engineering community to meet with each other and to exchange the latest ideas. This volume contains 35 revised and extended research articles written by experienced researchers participating in the conference. Well-known experts present their research on damage and fracture of material and structures, materials modeling and evaluation up to recent printing, and visualization for advanced analyses and evaluation.

The organizers and editors wish to thank all the authors for their participation and cooperation which made this volume possible. Finally, we would like to thank the team of Springer Publisher, especially Dr. Christoph Baumann, for the excellent cooperation during the preparation of this volume.

April 2015

Andreas Öchsner
Holm Altenbach

# Contents

# Effect of Alloying Elements on Corrosion, Microstructure and Mechanical Properties for Casted Free-Nickel Duplex Stainless Steels

**Ragaie Rashad, Amer E. Amer, Ahmed Y. Shash and Hany Shendy**

**Abstract** Free nickel Duplex stainless steels containing two different levels of 6–13 wt% manganese contents have been studied and analysed. The alloys, made up of appropriate mixtures of the alloying elements, Ferro-alloys and Ferro-alloys bearing nitrogen were melted in an induction furnace under nitrogen pressure. Even though the resistance to the pitting attack was controlled and enhanced by the nitrogen addition as well as, chromium, molybdenum contents. Also, the cast experimental alloy that contained high manganese was found to offer some advantages over the 2205-type duplex stainless steel in combination of mechanical properties and corrosion resistance. The microstructure development due to increasing manganese contents from 6 to 13 wt% revealed the decrease of the ferrite volume fraction from 82 to 75 %, respectively. Mechanical testing results showed that the free nickel alloys containing 0.14–0.23 wt% carbon with manganese contents ranging from 6.44 to 13.45 wt% have moderate mechanical properties whereas U.T.S. ranging from (691–815) MPa, Y.S. (585–738) MPa, elongation (19–21 %), and a corrosion rate of 0.044–6.0 mm/year, respectively. Manganese is

Ragaie Rashad: on Leave from Cairo University

R. Rashad
Department of Mechanical Engineering, British University in Egypt,
11837 P.O. Box 43, Cairo, Egypt
e-mail: Ragaie.Rashad@bue.edu.eg

A.E. Amer
Mechanical Design and Production Engineering Department,
Beni Suef University, Beni Suef, Egypt
e-mail: aeid958@yahoo.com

A.Y. Shash (✉)
Mechanical Design and Production Department, Faculty of Engineering,
Cairo University, Giza, Egypt
e-mail: ahmed.shash@cu.edu.eg

H. Shendy
The Egyptian Technical Military School, Cairo, Egypt
e-mail: shendy1969@yahoo.com



A. Öchsner and H. Altenbach (eds.), *Mechanical and Materials Engineering of Modern Structure and Component Design*, Advanced Structured Materials 70,
DOI 10.1007/978-3-319-19443-1_1

therefore an effective element of duplex microstructures. As an economical development, it is concluded that manganese is a useful replacement element for nickel in duplex alloys, but further work is required before the present alloys, or variations of them, could be commercially viable.

**Keywords** Free-Nickel duplex stainless steels · Corrosion resistance · Pitting attack · Microstructure development

## 1 Introduction

The industrial use of duplex stainless steel is rapidly increasing due to the combined advantages of better mechanical and corrosion properties [1–5]. Since the development of first-generation duplex stainless steels in the 1930s, considerable research efforts have been conducted to improve both mechanical and corrosion properties, particularly by controlling alloying elements, such as N, Cr, and Mo [3, 6–16]. Charles [4], for example, reported that the addition of Cr and/or Mo improved the resistance to pitting corrosion and stress corrosion cracking of duplex stainless steels. He further proposed that the addition of such elements needs to be done with caution since they can promote detrimental sigma phases at elevated temperatures [4]. Despite the extensive research works on the mechanical and corrosion behavior of duplex stainless steels, most of the researches have been conducted on the wrought products, and only a limited number of studies are available on the cast products of duplex stainless steels. Furthermore, Mn is often added to duplex stainless steel to increase the solubility of N to maximize the beneficial effect of N [17, 18]. According to the work of Gunn [19] and Kemp et al. [20] however, the effect of Mn on the microstructural evolution, as well as the mechanical and corrosion properties of duplex stainless steels have not been well established. The objective of the present study was therefore to examine the effect of Mn on the tensile and corrosion behaviour of free-nickel cast duplex stainless steels.

## 2 Experimental Procedures

The two experimentally proposed cast alloys of low and medium low carbon duplex stainless steel have been melted in a 10 kg laboratory induction furnace under nitrogen pressure around 8 bars and then cast in a metallic mould. The commercial duplex steels 2304 and 2205 grades were received in solution-annealed condition. The specimens were cut from plates and prepared for various property evaluations. The contents of alloying elements were determined, as shown in Table 1. The steels

**Table 1** Chemical composition of produced DSS

| Alloying elements | Low carbon samples | | DSS | |
|---|---|---|---|---|
| | Sample 1 | Sample 2 | 2304 | 2205 |
| C | 0.14 | 0.232 | 0.02 | 0.02 |
| Si | 0.27 | 0.288 | 0.31 | 0.32 |
| Mn | 6.44 | 13.45 | 1.5 | 1.5 |
| P | 0.0056 | 0.05 | 0.04 | 0.04 |
| S | 0.031 | 0.017 | 0.03 | 0.03 |
| Cr | 24.8 | 23.33 | 22.9 | 21.9 |
| Mo | 1.76 | 1.79 | 0.4 | 3.0 |
| Ni | 0.19 | 0.2 | 4.7 | 5.7 |
| N | 0.21 | 0.199 | – | – |

were heat treated by homogenization at 1200 °C for 6 h to decrease chemical segregation by diffusion and to homogenize the overall microstructure.

Test samples were solution annealed at 1050 °C for 15 min and then water quenched to dissolve inter-metallic phases and restore mechanical properties and corrosion resistance to the as-cast duplex stainless steel. In order to reveal the microstructure, the specimens were polished mechanically and then electro etched. The set up for the electro etching was 12 V, 20 °C and the electrolyte was solution of 10 % oxalic acid +2 % nitric acid. In addition, in order to evaluate quantitatively the duplex phases, EDX analysis attached to SEM microscopy was carried out to the solution annealed specimens. Tensile and hardness test samples were prepared and tested to measure the mechanical properties of the different alloys. Eventually, the corrosion resistance of the two samples of free nickel duplex stainless steel was measured by polarization tests and immersion tests, and the results were compared with the commercial duplex stainless steels as DSS 2304 and 2205. All polarization studies were carried out in a single component cell with three electrode configurations. A silver/silver chloride electrode saturated with KCl was used as a reference electrode and a platinum sheet with surface area of 1 $cm^2$ as a counter electrode. The electrochemical experiments were carried out under computer control using the potentiostat AUTOLAB® PGSTATE 30, where the working electrode was a 1 $cm^2$ specimen immersed in a 3.5 % NaCl solution. The immersion test where the variation of the corrosion rate for Nitrogen alloyed steel samples was done by measuring the weight loss per unit area with time in 10 wt% absolute HCl solution at room temperature. Prior to the immersion, the samples were mechanically polished using 400, 500 and 600 emery papers and lubricated using distilled water. The samples were then cleansed with distilled water, dried in air, weighed for the original weight ($W_o$) and then settled in the test solution. The corroded specimens were then removed from the solutions, cleansed with distilled water and dried, then the sample weight will be $W_1$ and the weight loss is ($W_o - W_1$). The corrosion attack was expressed in terms of weight loss per unit area (mg/$cm^2$).

# 3 Results and Discussion

## *3.1 Microstructural Evolution*

The microstructural features of cast DSS are significantly influenced by the type and amount of alloying elements and the heat treatment applied. The solidification mode and the morphology of the primary delta ferrite phase as a leading phase, depends mainly on composition. Solidification can begin with primary ferrite or primary austenite.

In general, the microstructure of the as-cast alloys solidifies into the two different morphologies: acicular or globular, according to the amount of interstitial austenitic stabilization elements as Carbon, Manganese and Nitrogen.

According to XRD analysis, the microstructure solidified to a globular structure consisting of approximately 80 % volume fraction of ferrite and consequently, the remaining volume is austenite and some inter-metallic compounds or carbides, as shown in Fig. 1. The effect of homogenization shows a more or less homogenous structure with the disappearance of non-metallic inclusions which was found before

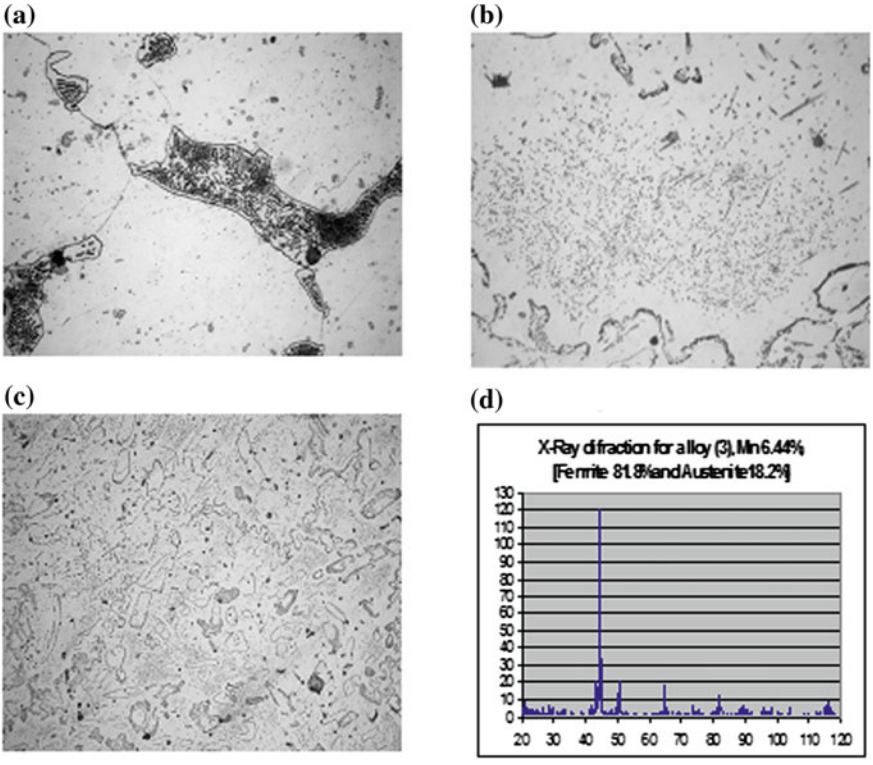


**Fig. 1** Microstructure of sample 1 containing 6.44 % Mn and 0.21 % N; **a** as cast, **b** homogenized, **c** solution annealed at 1050 °C, 30 min and **d** XRD analysis

as shown in Fig. 1a and b, respectively. Figure 1c illustrates the effect of the solution annealing treatment in dissolving the carbides and inter-metallic phases. On the other hand, the globular morphology is not modified even after solution annealing at 1050 °C.

As observed from Fig. 2, by increasing the manganese content, the amount of the austenite phase has a moderate increase and the structure had a ferrite volume structure of about 74 %, as investigated from the XRD analysis. Hence, improving in the tensile properties of that alloy was expected due to the increase of the amount of austenite phases compared with the previous commercial steel sample. Unfortunately, that improve in the mechanical properties was associated with a decrease in the corrosion resistance of this steel sample, as it will be discussed and mentioned later in the characterization and evaluation of corrosion properties. The role of homogenization annealing is still to modify the grains size to be more uniform and finer, decreasing the amount of non-metallic inclusion and chemical segregation by diffusion.

Table 2 shows the variation of ferrite volume fractions due to change of manganese contents.

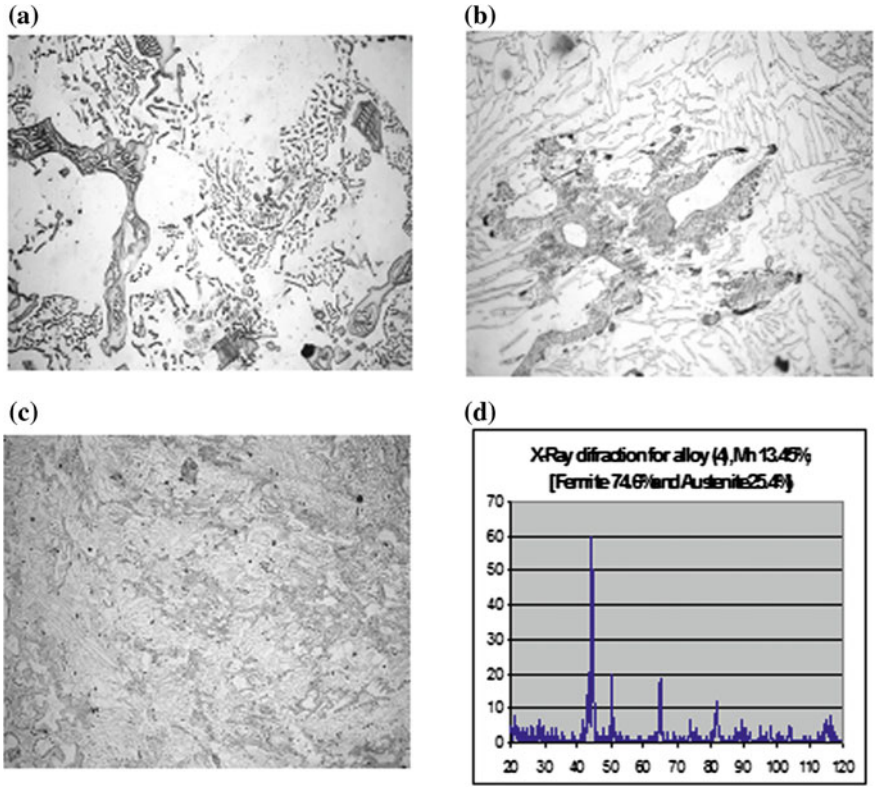


**Fig. 2** Microstructure of sample 2 containing 13.45 % Mn and 0.19 % N; **a** as cast, **b** homogenized, **c** solution annealed at 1050 °C, 30 min, and **d** XRD analysis

**Table 2** Characterization of phases by X-ray diffraction analysis

| Sample no. | 1 | 2 |
|---|---|---|
| Manganese content | 6.44 % Mn | 13.45 % Mn |
| Volume fraction of ferrite | 81.8 % | 74.6 % |

## *3.2 Mechanical Properties Evaluation*

Mn is often added to stainless steels as an austenitic stabilizer for the partitioning effect of N [20]. In the present study, it was evident and demonstrated that different Mn contents significantly affect the tensile behaviour of the cast free nickel duplex stainless steel, as well as the corrosion behaviour. With increasing Mn content, the strength level was greatly increased from 691 to 815 MPa, while the tensile elongation was not notably reduced. Such a complex trend observed in tensile properties with varying Mn contents may be largely related to the microstructural evolution in the present alloy, including the volume fraction of each phase and the shape and size of the austenitic phase, both primary and secondary, along with an intrinsic solid solution hardening effect of Mn. Since, the austenitic phase is a harder phase than the ferritic phase, and the increase in the volume fraction of austenite would improve the strength level of cast duplex stainless steel, the remarkable increase in the yield strength value of the investigated alloy with increasing Mn content from 6.44 to 13.5 % was therefore attributed to the increase in the volume fraction of the austenite phase from 18.2 to 25.4 %, as well as the solid solution hardening effect of Mn as was evident in Fig. 3. The ultimate tensile strength value appeared to be related to the ductility which represents the capability of plastic deformation. The complex trend associated with the ultimate tensile strength values observed in Table 3 was therefore believed to be due to the intrinsic hardening effect of Mn and the change in tensile properties with Mn content in comparison to the commercial DSS 2304 and 2205. The decrease in the elongation with increasing Mn content appeared to be dependent on the change in the shape of the primary and secondary austenitic phase.

The one major advantage of duplex stainless steels is their high yield strength. For high Mn DSS, the yield strength is increased but the ductility and toughness are reduced. Both Ni-free DSS exhibit yield strengths of at least 550 to 750 MPa in combination with an elongation to fracture of at least 20 %.

## *3.3 Corrosion Resistance Measurement*

Nitrogen increases the resistance to pitting corrosion, especially in combination with molybdenum.

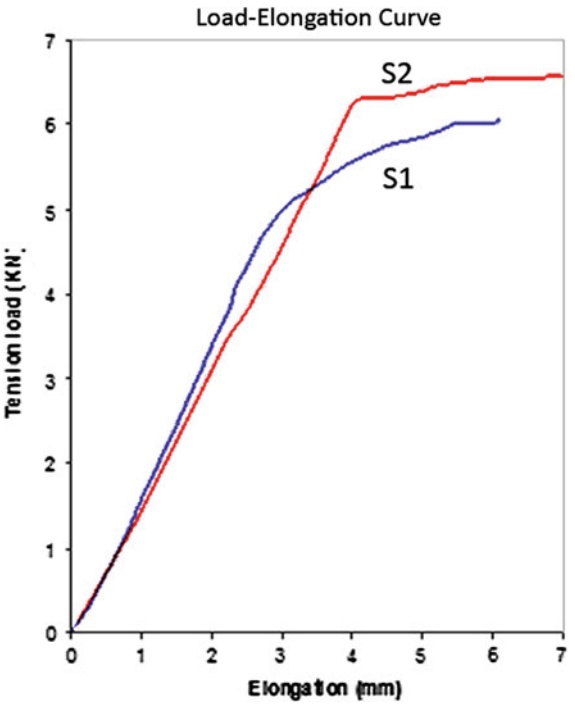


**Fig. 3** Load-elongation curve for Sample 1 and 2 with 6.44 and 13.45 wt% Mn, respectively

**Table 3** The results of mechanical properties of the experimental samples

| Sample no. | U.T.S. (MPa) | Y.S. (MPa) | Elong. (%) | Impact energy j | Brinell hardness (BHN) |
|---|---|---|---|---|---|
| 1 | 691 | 585 | 19 | 180 | 200 |
| 2 | 815 | 738 | 21 | 170 | 230 |
| DSS 2304 | 663 | 480 | 40 | 180 | 190 |
| DSS 2205 | 758 | 540 | 41 | 170 | 270 |

The Pitting Resistance Equivalent (PRE) was calculated according to the following equation [21]:

$$\mathrm{PRE} = \%\mathrm{Cr} + 3.3 \times \%\mathrm{Mo} + 20 \times \%\mathrm{N}$$

The pitting resistance results for samples 1 and 2 are illustrated in Table 4.

The polarizations resistance $R_p$ was measured by scanning the potential in a range between ±15 mV around the corrosion potential Ecorr at 0.1 mV/s. From the current density versus potential plot the reciprocal of the slope of the curve dE/dI was determined at the corrosion potential in resistance units (Ohm/cm$^2$).

**Table 4** PRE for samples 1 and 2

| Sample no. | Sample 1 | Sample 2 | Duplex 2304 |
|---|---|---|---|
| PRE | 33.01 | 33.17 | 35 |

The corrosion current densities in $\mu A/cm^2$ were calculated from the polarization resistance values using the Stern–Geary equation, [22]

$$I_{corr} = \frac{B_a \times B_c}{2.303(B_a + B_c)} \tag{1}$$

where the Tafel constants $B_a$ and $B_c$, are the slopes of tangents drawn on the respective anodic and cathodic polarization plots in mV/decade. Subsequently, the corrosion rate ($C_R$) was determined in mpy using the relationship:

$$C_R = \frac{0.13 \times I_{corr} \times eq.wt.}{\rho} \tag{2}$$

where ρ the density of the material ($g/cm^3$) and $I_{corr}$ the current density ($\mu A/cm^2$).

The $R_p$ is representative of the degree of protection of the passivation layer of the alloy surface. An increase in values of $R_p$ improves the corrosion resistance of steel. The corrosion characteristics ($R_p$, $I_{corr}$, $B_a$, $B_c$, $C_R$) were determined and the results summarized in Table 5. The values of $R_p$ allow a comparison scale to be established. The highest polarization resistances were revealed by S.1 of $2.94 \times 10^6$ $Ohm/cm^2$, while S.2 showed lower polarization resistances of $1.21 \times 103$ $Ohm/cm^2$. Based on the estimated $R_p$ values, it seems that the general corrosion behaviour of nitrogen–manganese stabilized austenitic steels is better than "conventional" steels of type 2304.

The Tafel slopes $B_c$, $B_a$ were determined by the fitting of a theoretical polarization curve to the experimental polarization curve plotted in the range of ±150 mV versus Eoc. The corrosion current Icorr is representative of the degree of degradation of the alloy. An alloy with a tendency towards passivity will have a value of $B_a$ greater than $B_c$, whereas an alloy that corrodes will have a $B_a$ lower than $B_c$. It can be noticed from Table 5, that regarding to the Tafel slope results, it was found that steels DSS 2304 and S.2 reveal a tendency towards depassivity. For S.1, $B_a$ is higher than $B_c$ indicating to passivation ability.

**Table 5** Comparison of the electrochemical quantities measured and calculated for the various steels (37 °C)

| Sample | $B_a$ | $B_c$ | $R_p$, (Ohm) | $I_{corr}$, ($\mu A/cm^2$) | $C_R$, (mpy) |
|---|---|---|---|---|---|
| DSS 2304 | 0.021 | 0.038 | 1.58E4 | 3.67 | 0.98 |
| S.1 | 0.039 | 0.027 | 2.94E6 | 0.15 | 0.044 |
| S.2 | 0.007 | 0.068 | 1.21E3 | 22.5 | 6.0 |

$B_c$ and $B_a$ tafel slopes, corrosion potential; $R_p$ polarization resistance; $I_{corr}$ corrosion current, $C_R$ corrosion rate

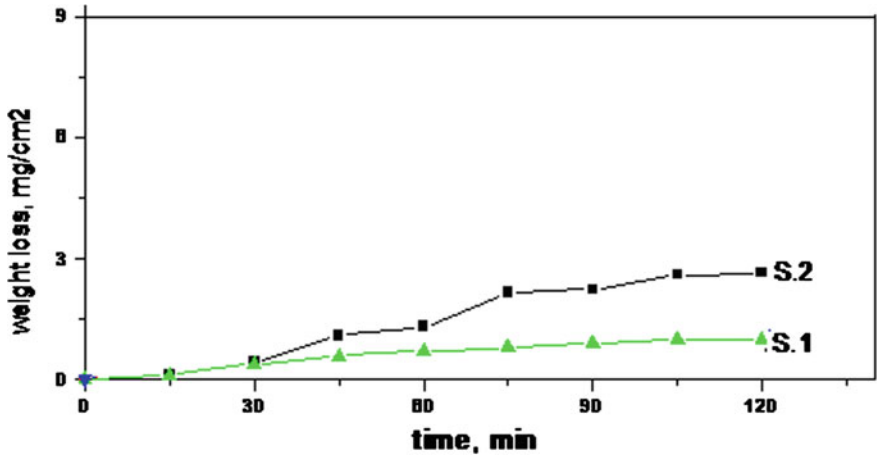


**Fig. 4** Corrosion rate versus exposure time in 10 wt% HCl

Generally, the corrosion behavior of nitrogen–manganese stabilized austenitic steels S.1 is better than S.2.

The weight losses of Duplex Stainless Steel alloys in 10 %wt HCl have been determined as a function of the immersion time. The tested sample was immersed at room temperature in 10 %wt HCl for various immersion periods (0–120 min). The variation of the corroded weight (weight loss) with immersion time is shown in Fig. 4. It is obvious that the weight loss $W_{loss}$ (mg/cm$^2$) increased linearly with immersion time.

The resistance to pitting corrosion is associated with nonmetallic inclusions present in the alloys. Alloys S.1 and S.2 are more pitting resistance due to their low carbon content of 0.14 and 0.232 %, respectively. The data indicated that the annual corrosion rate of S.1 was the lowest due to probably its highest Mn content, i.e. the increase in Mn content of the alloys decreased the resistance to pitting corrosion. It can be concluded that the results of electrochemical polarization and immersion tests are coincident.

## 4 Conclusion

Two kinds of nickel-free duplex stainless steels have been developed in this scientific research work. These alloys can be characterized by their high strength and toughness, good corrosion resistance and low alloy element cost. In comparison with the commercial DSS with a similar $PRE_N$, the experimental DSS have a higher yield strength by roughly 100–200 MPa and a lower elongation to fracture of about 20 %. The increase in yield strength and ultimate tensile strength value of the investigated alloy with increasing Mn content from 6.44 to 13.5 % was therefore

attributed to the increase in the volume fraction of the austenite phase from 18.2 to 25.4 %, as well as the solid solution hardening effect of Mn. Microstructural investigations showed that such alloys have relatively stable austenite content at high temperatures. Due to the absence of nickel, the experimental DSS exhibit an excellent resistance to SCC in chloride solutions. Finally, these alloys can be cost-efficient because of the total absence of the expensive element nickel and therefore can find applications where high strength and moderate corrosive resistance are required.

**Acknowledgments** The authors would like to thank the late Prof. Dr.-Ing. Y. Shash the Head of the Mechanical Design and Production Department, Faculty of Engineering, Cairo University for his kind support and wise scientific advices. Thanks goes to Dr. A. Abd Elaal from Department of Metals Technology, Central Metallurgical Research and Development "CMRDI", Helwan-Cairo Egypt for the corrosion tests.

## References

1. Huang J, Altstetter C (1995) Cracking of duplex stainless steel due to dissolved hydrogen. Metall Mater Trans A 26A:1079–1085
2. Davis J (1996) ASM specialty handbook stainless steels. ASM International, Materials Park, OH, pp 32
3. Solomon H, Devine T (1983) In: Lula RA (ed) Duplex stainless steels. ASM, Metals Park, OH, pp 693
4. Charles J (1994) In: Proceedings of the fourth international conference on duplex stainless steels, vol 1. Paper KI, Glasgow
5. Nicholls J (1994) In: Proceedings of the fourth international conference on duplex stainless steels, vol 1. Paper KIII, Glasgow
6. Son J, Kim S, Lee J, Choi B (2003) Effect of N addition on tensile and corrosion behaviors of CD4MCU cast duplex stainless steels. Metall Mater Trans A 34A:1617
7. Son J, Kim S, Lee J, Choi B (2002) Slow strain rate tensile behavior of CD4MCU cast duplex stainless steel with different nitrogen contents. J Korean Inst Met Mater 40:723
8. Park Y, Lee Z (2001) The effect of nitrogen and heat treatment on the microstructure and tensile properties of 25Cr–7Ni– 1.5Mo–3W–xN duplex stainless steel castings. Mater Sci Eng A 297:78
9. Son J, Kim S, Lee J, Choi B (2003) Tensile and Corrosion Behaviors of As-solutionized CD4MCU Cast Duplex Stainless Steel with Different Nitrogen Contents. J Korean Inst Met Mater 40:949
10. Sakai J, Matsushima I, Kamemura Y, Tanimura M, Osuka T (1983) In: Lula RA (ed) Duplex stainless steels. ASM, Metals Park, OH, pp 211
11. Kim S, Paik K, Kim Y (1998) Effect of Mo substitution by W on high temperature embrittlement characteristics in duplex stainless steels. Mater Sci Eng A 247:67
12. Poznansky A, Nalbone C, Crawford J (1983) In: Lula RA (ed) Duplex stainless steels. ASM, Metals Park, OH, pp 431
13. Kim J, Park C, Kwon H (1999) Bull Korean Inst Met Mater 12:635
14. Guha P, Clark C (1983) In: Lula RA (ed) Duplex stainless steels. ASM, Metals Park, OH, pp 355
15. Okazaki Y, Miyahara K, Hosoi Y, Tanino M, Komatsu H (1989) Effect of alloying elements of σ phase formation in Fe-Cr-Mn alloys. J Jpn Inst Met 53:512

16. Speidel M (1991) In: Proceedings of the international conference on stainless steels, vol 1. ISIJ, Chiba, p 25
17. Nilsson J (1992) Superduplex stainless steels. Mater Sci Technol 8:685
18. Merello R, Botana F, Botella J, Matres M, Marcos M (2003) Influence of chemical composition on the pitting corrosion resistance of non-standard low-Ni high-Mn-N duplex stainless steels. Corros Sci 45:909
19. Gunn R (1997) Duplex stainless steel. Abington, Cambridge, p 15
20. Kemp AR, Dekker NW, Trinchero P (1995) Differences in inelastic properties of steel and composite beams. J Constr Steel Res 34:187–206
21. Gunn R (ed) (1997) Duplex stainless steels—microstructure, properties, and applications. Abington Publishing, Cambridge
22. Stern M, Geary A (1957) Electrochemical polarization: I. A theoretical analysis of the shape of polarization curves. Electrochem J 56–63

# Influence of $Al_2O_3$ Nano-dispersions on Mechanical and Wear Resistance Properties of Semisolid Cast A356 Al Alloy

**Ahmed Y. Shash, Amer E. Amer and Moataz El-Saeed**

**Abstract** The present investigation studies the prospects of using nanoparticles as reinforcement ceramic powders to gain improved performance of A356 Al cast alloy. Alumina nano-powder of 40 nm size was stirred into the A356 matrix with different fraction ratios ranging from (0, 1, 2 and 4 wt%) in a mushy zone (600 °C) using a constant stirring time for one minute. To evaluate the results, the alloys were further characterized by various tribological and mechanical characterization methods. The results showed higher strength values with improved ductility when compared to the monolithic alloy under the same casting conditions. Also, the wear resistance has been positively enhanced as the amount of the $Al_2O_3$ nano-particles addition increases from 1 to 4 wt% leading to a decrease in the weight loss ranging from 5.5 to 4.0 mg, respectively. The Scanning Electron Microscopy of the fracture surface and the wear surface revealed the presence of nanoparticles at the inter-dendritic space of the fracture surface and was confirmed with an EDX analysis of these particles.

**Keywords** Nano-metal matrix composites · $Al_2O_3$ nano-powders · Wear resistance · Mushy zone · Mechanical stirring

A.Y. Shash (✉)
Mechanical Design and Production Department, Faculty of Engineering,
Cairo University, Giza, Egypt
e-mail: ahmed.shash@cu.edu.eg

A.E. Amer
Mechanical Design and Production Engineering Department, Beni Suef University,
Beni Suef, Egypt
e-mail: aeid958@yahoo.com

M. El-Saeed
Department of Mechanical Engineering, Akhbar El-Youm Academy, 6 of October City,
Giza, Egypt
e-mail: mo3taz.elsaeed@gmail.com



A. Öchsner and H. Altenbach (eds.), *Mechanical and Materials Engineering of Modern Structure and Component Design*, Advanced Structured Materials 70,
DOI 10.1007/978-3-319-19443-1_2

## 1 Introduction

History is often marked by the materials and technologies that reflect human capabilities and understanding. Many time scales begins with the stone age, which led to the Bronze, Iron, Steel, Aluminum and Alloy age, as improvements in refining and smelting took place and science made it possible to move towards finding more advanced materials. Composite structures have shown universal savings of at least 20 % over metal counterparts and a lower operational and maintenance cost [1]. Aluminum based alloys and metal matrix composites (MMCs) exhibit attractive tribological and mechanical properties such as a high specific modulus, good strength, long fatigue life, superior wear resistance and improved thermal stability, which allow these alloys to have numerous applications in the aerospace, automobile and military industries. As the data on the service life of composite structures is becoming available, it can be safely said that they are durable, maintain dimensional integrity, resist fatigue loading and are easily maintainable and repairable. Composites will continue to find new applications, but the large scale growth in the marketplace for these materials will require less costly processing methods and the prospect of recycling [2] will have to be solved [3].

Composite materials are emerging chiefly in response to unprecedented demands from technology due to rapidly advancing activities in aircrafts, aerospace and automotive industries. These materials have low specific gravity that makes their properties particularly superior in strength and modulus to many traditional engineering materials such as metals. As a result of intensive studies into the fundamental nature of materials and better understanding of their structure property relationship, it has become possible to develop new composite materials with improved physical and mechanical properties [4–6]. These new materials include high performance composites such as polymer matrix composites, ceramic matrix composites and metal matrix composites etc. Continuous advancements have led to the use of composite materials in more and more diverse applications. The importance of composites as engineering materials is reflected by the fact that out of over 1600 engineering materials available in the market today more than 200 are composites [6].

For most applications, a homogeneous distribution of the particles is desirable in order to maximize the mechanical properties [5]. In order to achieve a good homogeneous distribution of a particle in the matrix, the process parameters related with the stir casting method must be studied [4, 5]. So that it is essential to study the influence of stirring speed and stirring time on the distribution of particles in MMC.

In the Prabu [7] study, the stirring speeds were set at 500, 600 and 700 rpm and the stirring times were set at 5, 10 and 15 min for this study.

Many researchers have claimed enhanced properties for these produced composites relative to those produced by reinforcing with micro-particles.

Therefore the aim of this research work is to improve the mechanical and tribological properties of the A356 aluminum alloy using ceramics $Al_2O_3$ nano particles.

## 2 Experimental Procedures

The experimental work carried out through this scientific study consists of the following three stages:

(a) Production of new NMMC alloys.
(b) Identification of the mechanical and wear resistance properties.
(c) Characterization of the new material.

### *2.1 Materials Produced*

The hypoeutectic alloy A356 was used as a base metal for the produced material having the chemical composition shown in Table 1. The material used for reinforcement was 1, 2, and 4 % by weight $Al_2O_3$ ceramic nano-particles with constant particle size of 40 nm, the description of which is given in Table 2.

### *2.2 Equipments Used*

#### 2.2.1 Melting Furnace

An electric resistance furnace was designed and constructed for approaching this research work for preparing the NMMCs. It consists of a lift out ceramic crucible of max. 2 kg, a heating system, and is connected to a stirring mechanism with a

**Table 1** Chemical composition (in wt%) of A356 cast Al–Si

| Alloy | Chemical composition (wt%) | | | | | | | |
|---|---|---|---|---|---|---|---|---|
| | Al | Si | Mg | Fe | Cu | Pb | Zn | Mn |
| A356 | Bal. | 7.44 | 0.3 | 0.27 | 0.02 | 0.022 | 0.01 | Nil |

**Table 2** Properties of $Al_2O_3$ reinforcement powders

| Reinforcement | $\gamma$-$Al_2O_3$ |
|---|---|
| Density (solid) (g/cm$^3$) | 3.95 |
| Crystal structure | FCC |
| Appearance | White solid |
| Young's modulus (GPa) | 380 |
| Average size (nm) | 40 |
| Melting point | 2054 °C |

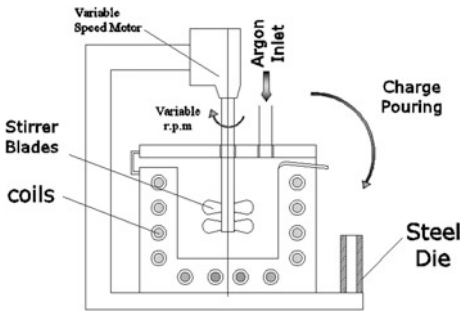


**Fig. 1** Schematic apparatus used for preparing the NMMCs

3000 rpm max. rotating speed motor and adjustable height with a control unit of up to 1200 °C connected to a thermocouple for controlling the stirring temperature Fig. 1.

### 2.2.2 Metallic Mould

The melt was poured into a mild steel mould, in which the casted samples were in a 24 mm diameter as shown in Fig. 2.

## *2.3 Melting Methodology and Approach*

A charge of 0.5 kg of the A356 alloy was introduced to the crucible and heated up to the melting temperature (640 °C). The melt was degassed and shielded with argon before pouring after reaching the liquid state to prevent oxidation of the molten metal. The melt was subsequently brought down to the semi-solid state by around 605 °C and hence the $Al_2O_3$ nano-powders were preheated to 700 °C and then added to the melt simultaneously with mechanical stirring for 1 min at 1500 rpm. The fabrication conditions of the composites prepared in this investigation are

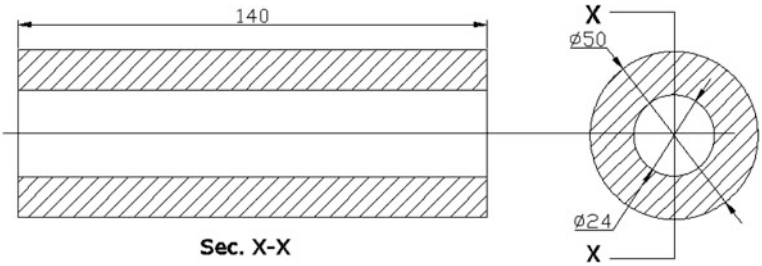


**Fig. 2** Schematic drawing for the mould used

**Table 3** List of produced alloys and fabrication conditions

| Melt no. | Additions | Stirring (rpm) | Pouring temp. (semi-solid) |
|---|---|---|---|
| Melt 1 | A356 | 1500 | 605 °C |
| Melt 2 | A356 + 1 % $Al_2O_3$ | 1500 | 605 °C |
| Melt 3 | A356 + 2 % $Al_2O_3$ | 1500 | 605 °C |
| Melt 4 | A356 + 4 % $Al_2O_3$ | 1500 | 605 °C |

summarized in Table 3. Cast samples were poured into the prepared mould without additions and with additions of the different investigated $Al_2O_3$ percentages.

## *2.4 Mechanical Properties*

Mechanical properties, mainly tensile strength, ductility, hardness and wear resistance, were determined in the as-cast conditions for the investigated NMMC samples.

### 2.4.1 Tensile Test

The tensile tests were conducted on round tension test specimens of diameter 5.02 mm and gage length 25.2 mm using a universal testing machine according to DIN 50125. The elongation percentage and ultimate tensile strength were calculated. The results were based on the average of three samples taken from each melt.

### 2.4.2 Hardness Test

The hardness tests were conducted on Rockwell hardness testing machines in the Faculty of Engineering, Cairo University, using a $(\frac{1}{16})''$ diameter hardened steel ball and a 62.5 kg applied load. The reported results are the average of three readings for each case.

### 2.4.3 Wear Test

A PLINT TE 79 Multi Axis Tribometer Machine was used for measuring friction force; friction coefficient and wear rate for NMMC manufactured materials, as illustrated in Fig. 3, in which a standard specimen with a diameter of 8 and 20 mm length as a computerized pin on disc machine used for friction and wear testing of materials is loaded vertically downwards onto the horizontal disc.

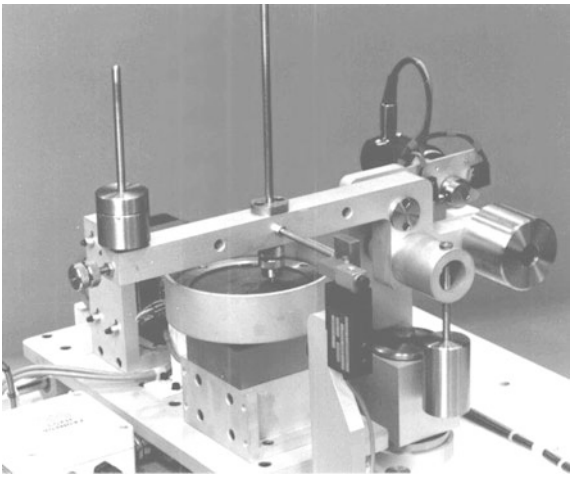

**Fig. 3** PLINT TE 79 multi axis tribometer machine

## *2.5 Material Characterization*

### 2.5.1 Microstructural Evolution

Representative sections from the cast samples were cut into 3 pieces: the 1st from the top, the 2nd from the middle and the 3rd from the bottom. Samples were wet grounded on a rotating disc using silicon carbide abrasive discs of increasing fineness (120, 180, 220, 320, 400, 600, 800, 1000 and 1200 grit). Then they were polished using 10 μm alumina paste.

### 2.5.2 Optical Microscopy (OM)

The microstructure examination was carried out using an OLYMPUS DP12 optical metallurgical microscope, equipped with a high resolution digital camera for the investigation of the microstructure.

### 2.5.3 Scanning Electron Microscope (SEM)

The surface topography and the fracture characteristics were studied using SEM to understand the fracture mechanism and also to detect the favorable sites for particle incorporation by using a JSM-5410 Scanning Electron.

The JSM-5410 scanning electron microscope is a high-performance multipurpose SEM with a high-resolution of 3.5 nm, and EDXS (energy dispersive X-ray spectrometer). Its automated features included Auto Focus/Auto Stigmator, and Automatic Contrast and Brightness. The EDS makes the JSM-5410 expandable from morphological observations to multi-purpose high-resolution elemental analysis.

# 3 Results and Discussions

## *3.1 Mechanical Properties of the NMMC*

Table 4 illustrates the mechanical properties (tensile strength, elongation in %, and hardness) of the produced castings with reinforced $Al_2O_3$ nanopowder.

As can be seen from Fig. 4, as the wt% fraction of $Al_2O_3$ nanopowder increases the UTS increases reaching 195 MPa, until a value of 2 wt% of $Al_2O_3$. Beyond this weight fraction, the UTS decreases as the wt% increases.

As shown in Fig. 5, increasing the weight fraction of $Al_2O_3$ has no visible effect on ductility until reaching 1 wt%, then with increasing the wt% beyond 1 wt% the ductility increases. The ductility of NMMC increases by about 40 % at 2 wt% of $Al_2O_3$ nanopowder. At 4 wt% fraction, the ductility reaches to its minimum values; due to the agglomeration of the dispersed particles in the NMMC, while its hardness at this weight fraction increases by about 30 % as shown in Fig. 6. The presence of the ceramic phase increases the hardness of the alloys and hence, reduces the ductility of the composites in comparison with the matrix alloy.

Substantial increases in strength, along with good ductility, have been observed in a number of alloys with multiphase nanoscale microstructures.

**Table 4** Mechanical properties (tensile strength, elongation in % and hardness) NMMC using $Al_2O_3$ Nanopowder

| Melt no. | Additions | UTS (MPa) | Elongation % | Hardness RB |
|---|---|---|---|---|
| Melt 1 | A356 | 155 | 5 | 57 |
| Melt 2 | A356 + 1 % $Al_2O_3$ | 170 | 5 | 61 |
| Melt 3 | A356 + 2 % $Al_2O_3$ | 195 | 6.8 | 72 |
| Melt 4 | A356 + 4 % $Al_2O_3$ | 163 | 4.2 | 73 |

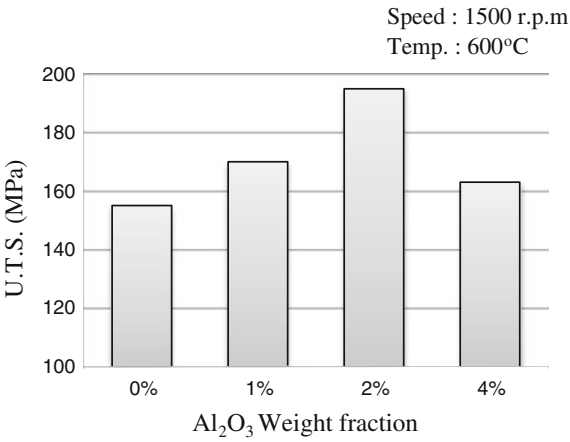


**Fig. 4** The effect of wt% fraction of $Al_2O_3$ nanopowder on the ultimate tensile strength of MMC at 1500 rpm stirring speed at a semi-solid-state (600 °C)

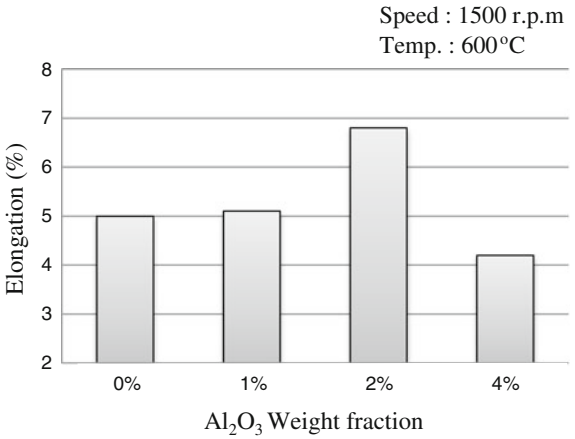


**Fig. 5** The effect of wt% fraction of $Al_2O_3$ nanopowder on elongation % of MMC at 1500 rpm stirring speed when in a semi-solid state (600 °C)

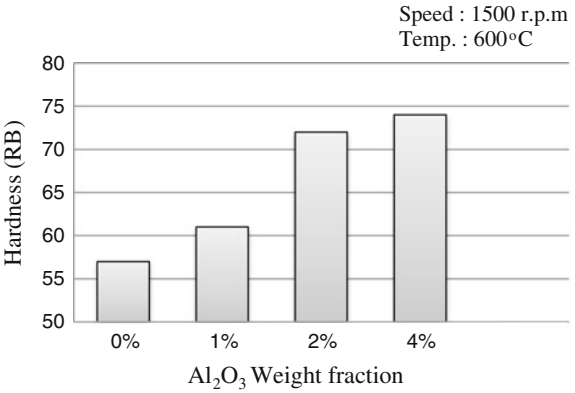


**Fig. 6** The effect of wt% fraction of $Al_2O_3$ nanopowder on the hardness of MMC at 1500 rpm stirring speed when in a semi-solid state (600 °C)

These properties originate from the fine distribution of globular particles in an A356 matrix on a nanometer scale, where the globular particles act as strength bearing components, while the A356 matrix supplies ductility. The existence of a crystalline approximant phase at the interface between the particles and the FCC Al matrix improves interfacial bonding between the different phases, thus important for the combination of high strength and good ductility without failure at the interface [8].

The wear tests were then performed with the following parameters: velocity = 0.8 m/s, time = 1200 s and load = 10 N.

The average wear results of A356 samples reinforced with 0, 1, 2 and 4 wt% $Al_2O_3$ nanopowder are shown in Table 5.

As was expected from the results shown in Table 5 that the wear resistance increases as the weight percentage of the reinforced nano particles increases.